7); perhaps markers commonly deleted in other genitourinary tract neoplasms may facilitate the detection of other neoplasms that exfoliate cells into urine sediment.

Finally, our approach highlights the immediate utility of studies that demonstrate LOH in human cancer and of the development of molecular progression models for clinical detection (*18*). In most of the cases in this study, morphologic and cytologic analyses were not diagnostic. Molecular analysis reliably detected tumors of all grades and stages, including those often missed by cytology. In principle, this molecular approach can be performed at approximately one-third the cost of cytology and does not require exhaustive expert interpretation. Moreover, the entire assay is amenable to nonradioactive, non–gel separation techniques (*19*) and potentially could lead to a reliable, yet inexpensive, molecular screening test.

REFERENCES AND NOTES

1. C. C. Boring, T. S. Squires, T. Tong, *Cancer J. Clin.* **45**, 8 (1995).
2. G. N. Papanicolaou and V. F. Marshall, *Science* **101**, 519 (1945).
3. G. M. Farrow, D. C. Utz, C. C. Rife, *Cancer Res.* **36**, 2495 (1976); W. M. Murphy, M. S. Soloway, A. F. Jukkola, W. N. Crabtree, K. S. Ford, *Cancer (Philadelphia)* **53**, 1555 (1984); C. T. Sarnacki *et al.*, *J. Urol.* **106**, 761 (1971); M. N. El-Bolkainy, *ibid.* **124**, 20 (1980).
4. S. C. Hopkins, K. S. Ford, M. S. Soloway, *J. Urol.* **130**, 61 (1983).
5. A. A. Sandberg, *Cancer Genet. Cytogenet.* **19**(1–2), 163 (1986); E. R. Fearon, A. P. Feinberg, S. H. Hamilton, B. Vogelstein, *Nature* **318**, 377 (1985); Y. C. Tsai *et al.*, *Cancer Res.* **50**, 44 (1990); S.-Q. Wu *et al.*, *ibid.* **51**, 3323 (1991); D. Sidransky and E. Messing, *Urol. Clin. North Am.* **19**, 629 (1992).
6. D. Sidransky *et al.*, *Science* **252**, 706 (1991); R. H. Hruban, P. van der Riet, Y. S. Erozan, D. Sidransky, *N. Engl. J. Med.* **330**, 1276 (1994).
7. D. Sidransky *et al.*, *Science* **256**, 102 (1992); L. Mao, R. H. Hruban, J. O. Boyle, M. Tockman, D. Sidransky, *Cancer Res.* **54**, 1634 (1994).
8. L. Mao *et al.*, *Proc. Natl. Acad. Sci. U.S.A.* **91**, 9871 (1994).
9. Frozen tumor tissue was cut into 10-μm sections. All samples (including lymphocytes) were digested with 1% SDS–proteinase K at 60°C for 5 hours, and DNA was extracted by ethanol precipitation. Urine samples were spun at 3000*g* for 5 min and washed twice with phosphate-buffered saline. Each PCR mixture (25 μl) contained 50 ng of DNA template. Primers were obtained from Research Genetics (Huntsville, AL) or synthesized from sequences in the Genome Database (GDB). For microsatellite analysis, one primer was labeled with T4 polynucleotide kinase (New England Biolabs) and [γ-^{32}P]-adenosine triphosphate (New England Nuclear). Microsatellite loci and primer sequences are available from the authors on request. DNA was subjected to 30 to 35 cycles of amplification in a Hybaid (Middlesex, UK) Omnigene TR3 SM2 Thermocycler as follows: 95°C for 30 s, 52° to 60°C for 1 min, and 72°C for 1 min, with a final extension step of 72°C for 5 min. PCR products were separated by electrophoresis in denaturing 8 M urea-polyacrylamide-formamide gels, which were then subjected to autoradiography (*8*).
10. We tabulated the total alterations for each marker tested in all tumors and then grouped, in descending order, the markers most susceptible to alterations that would empirically detect the greatest number of primary tumors. Thus, the 10 most susceptible markers empirically identified at least one alteration in 26 of 50 tumors (52%), 11 identified 56% of tumors, 12 identified 60%, 13 identified 62%, and so forth. Some markers identified alterations only in tumors previously identified by another marker, and 20% of tumors did not demonstrate a single alteration with any marker tested.
11. P. Cairns *et al.*, *Nature Genet.* **11**, 210 (1995).
12. Approximately 50 cm^3 of urine was obtained and concentrated by centrifugation on cytospin glass slides or Millipore filters (Burlington, MA). Cells were stained by Papanicolaou stain and visualized under microscopy. Samples were initially screened by a cytotechnologist and reviewed by a cytopathologist. Standard morphologic criteria were used to establish the presence of neoplastic cells.
13. L. L. Wheeless *et al.*, *Cytometry* **17**, 319 (1994); L. E. Moore, N. Titenko-Holland, M. T. Smith, *Environ. Mol. Mutagen.* **22**(3), 130 (1993).
14. D. Sidransky *et al.*, *N. Engl. J. Med.* **326**, 737 (1992).
15. G. T. Williams, *Cell* **65**, 1097 (1991); D. E. Fisher, *ibid.* **78**, 539 (1994).
16. E. Ruoslahti and J. C. Reed, *ibid.* **77**, 477 (1994).
17. M. A. Knowles *et al.*, *Cancer Res.* **54**, 531 (1994); W. Y.-H. Chang, P. Cairns, M. P. Schoenberg, T. J. Polasick, D. Sidransky, *ibid.* **55**, 3246 (1995); M. P. Rosin, P. Cairns, J. I. Epstein, M. P. Schoenberg, D. Sidransky, *ibid.*, p. 5213.
18. E. Fearon and B. Vogelstein, *Cell* **61**, 759 (1990).
19. H. M. Wenz, *Nucleic Acids Res.* **22**, 4002 (1994).
20. O. H. Beahrs, D. E. Henson, R. V. P. Hutter, M. H. Myers, Eds., *Manual for Staging of Cancer* (Lippincott, Philadelphia, ed. 3, 1988), p. 27.

21. Oncor Inc. (Gaithersburg, MD) provided research funding for this study. Under an agreement between Oncor and Johns Hopkins University, D.S. is entitled to a share of sales royalty received by the university from Oncor. Under that agreement, the university and D.S. also have received Oncor stock, which, under university policy, cannot be traded until 2 years after the first commercial sales of the products related to this research. D.S. also serves as a member of the Scientific Advisory Board of OncorMed Inc., an Oncor subsidiary, which is commercializing some of Oncor's technology. The terms of this arrangement have been reviewed and approved by the university in accordance with its conflict-of-interest policies.

14 September 1995; accepted 6 December 1995

Expression of a *Plasmodium* Gene Introduced into Subtelomeric Regions of *Plasmodium berghei* Chromosomes

Melissa R. van Dijk, Chris J. Janse, Andrew P. Waters*

Targeted integration of exogenous DNA into the genome of malaria parasites will allow their phenotype to be modulated by means of gene disruption or the stable expression of foreign and mutated genes. Described here is the site-specific integration through reciprocal exchange, and subsequent expression, of a selectable marker gene into the genome of the pathogenic, bloodstage forms of the rodent malaria parasite *Plasmodium berghei*. Stable integration of a single copy of the marker gene (retained for more than 70 generations in the absence of drug pressure) into a nontranscribed subtelomeric repeat array of different chromosomes was observed. Expression of the gene within the subtelomeres indicated that the previously recorded absence of transcription in these regions could be due to a corresponding absence of genes rather than active silencing mechanisms.

Systems enabling the genetic manipulation of malaria parasites will play a crucial role in furthering our understanding of the biology of these protozoa. In turn, this knowledge might contribute to improved rationales for the combat of the disease. Targeted insertion of foreign DNA into the malaria parasite genome will permit the examination of the function of parasite genes and the reintroduction of mutated forms of those same genes. The successful introduction of functional plasmid DNA into malaria parasites has been demonstrated in both transient (*1*) and stable (*2*) procedures, but neither random nor site-directed integration of the introduced DNA into the *Plasmodium* genome has been reported.

We have previously shown that it is possible to stably introduce plasmid DNA containing the gene encoding the bifunctional enzyme dihydrofolate–thymidylate synthase (DHFR-TS) (which confers resistance to the drug pyrimethamine) and additional parasite DNA into bloodstages of *Plasmodium berghei* (*2*). When two different plasmids (pMD223 and pMD221) with the potential to integrate into the genome were introduced in both circular and linear forms, we observed only drug-resistant, transformed parasites that maintained the plasmids episomally. In the experiments described here we introduced linearized pMD223 containing an internal 2.2-kb portion of a 2.3-kb repeat element. This 2.3-kb element is a nontranscribed repetitive DNA sequence specific to the rodent malaria parasite *P. berghei*. It is present in a total copy number of 200 to 300 in the genome, arranged as a head-to-tail array, and located exclusively in the subtelomeric regions of several chromosomes (*3*). Plasmid pMD223 was linearized at a unique Spe I site present in the 2.3-kb repeat. In four separate experiments (T6, T7, T8, and T9), the linear form of pMD223 was electro-

Department of Parasitology, University of Leiden, 2300 AL Leiden, Netherlands.

*To whom correspondence should be addressed.

porated into 10^9 merozoites of the drug-sensitive clone 15cy1, followed by selection for pyrimethamine resistance (*2*). Stable, drug-resistant parasites were recovered in all instances (T6, T7, T8, and T9 parental lines). Parasites from the T6 and T9 lines were cloned by limiting dilution, and we obtained three clones from T6 (examples discussed, T6.1 and T6.2) and nine clones from T9 (examples discussed, T9.1 and T9.2). All parasite lines and clones from these experiments were highly resistant to pyrimethamine. The IC_{50} values (the 50% inhibitory concentration) for pyrimethamine, as determined in vitro (*2*), were 530 to 930 times the IC_{50} values of the sensitive parent clone 15cy1 (T6.1, 530×; T6.2, 920×; T7, 930×; T8, 920×; and T9, 530×). This level of resistance is comparable with the high level of resistance observed in *P. berghei* parasites that contain the amino acid substitution $Ser^{110} \rightarrow Asn$ in the chromosomal copy of the DHFR-TS gene (*4*). Polymerase chain reaction analysis of all transformed parasites indicated that pMD223 DNA was present (*5*).

Chromosomes from the four parental lines were separated by clamped homogenous electric fields (CHEF) gel electrophoresis, transferred to nylon membranes, and hybridized to probes for the DHFR-TS gene and the vector (pBSKS) (Fig. 1, A and B). As expected, all lines showed a positive signal with the DHFR-TS probe to chromosome 7 where the parental, centromeric copy of the DHFR-TS gene is located. In addition, the combination of hybridization signals suggested that an additional DHFR-TS gene linked to plasmid DNA was integrated into chromosome 7 (T6), chromosomes 13/14 (T7 and T8), and both chromosome 7 and 13/14 (T9). Chromosomes 7 and 13/14 of the parental, drug-sensitive clone 15cy1 contain the highest copy number of the 2.3-kb repeat target (*3*). The T9 parental line consisted of a mixture of parasites, with pMD223 integrated either in chromosome 7 (T9.2) or in chromosome group 13/14 (T9.1) (*5*). The clones from the T6 population (T6.1 and T6.2) both contained the extra copy of DHFR-TS gene in chromosome 7.

The digestion of purified chromosome 7 of clones T6.1, T6.2, and T9.2 with Apa I and hybridization to the DHFR-TS probe confirmed the presence of an extra, integrated copy of the DHFR-TS gene on this chromosome in addition to the normal copy that lies on a 270-kb internal fragment (Fig. 1, C to E, H, and I). Further hybridization of the restriction fragments to a telomeric probe indicated that the additional DHFR-TS gene was located on a telomeric fragment of the chromosome. Similar analysis of the chromosomes 13/14 from the T7, T8, and T9 lines and clone T9.1 showed that integrated copies of the DHFR-TS gene were also located on telomeric fragments (Fig. 1, F and G). The T7 and T8 populations were heterogenous, indicating that integration could have occurred in either chromosome 13 or 14, or both. Because of the difficulty of resolving these two chromosomes by electrophoresis, no further attempt was made to analyze these populations.

The whole chromosome analyses indicated that, in T6, integration of the vector occurred without a noticeable reduction in size of chromosome 7; however, the Apa I restriction fragment containing the integrated vector showed a slight size reduction. These data are consistent with site-directed integration into the 2.3-kb repeat arrays through a reciprocal exchange event spanning and deleting a small number of the tandem repeats. However, in T9 (for example, clone T9.2), integration into chromosome 7 was associated with a larger (~100-kb) reduction in size of the subtelomeric Apa I restriction fragment. This suggested one of the following: (i) The reciprocal exchange event spanned and deleted many 2.3-kb units within the tandem array. (ii) A single nonreciprocal exchange occurred followed by telomere addition with a resultant shortening of the target chromosome. (iii) The integration proceeded normally, and there was a secondary deletion of a variable number of 2.3-kb repeats. The internal Apa I fragments of the smaller form of chromo-

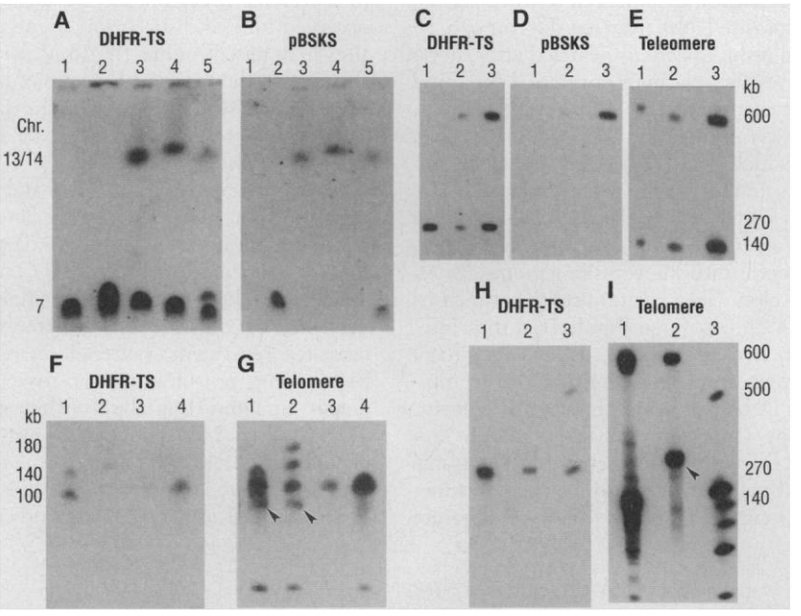

Fig. 1. Chromosome analysis of drug-resistant *P. berghei* parasites that were transformed with linear pMD223. (**A** and **B**) Analysis of the location of pMD223 in parasite chromosomes of parental populations of transformed parasites. Chromosomes of the parasites from experiments T6 through T9 were separated by CHEF, transferred to nylon filters, and hybridized to (A) the DHFR-TS probe or (B) the pBSKS probe. Film autoradiograms are shown. Probe labeling and hybridization were as described (*2*). CHEF conditions were as follows: first run, 60 hours, 3.5 V cm^{-1}, pulse time from 500 to 700 s; second run, 25 hours, 3.5 V cm^{-1}, pulse time 300 to 500 s; and third run: 8 hours, 3.5 V cm^{-1}, pulse time from 200 to 300 s. Lane 1, clone 15cy1; lanes 2 to 5, T6 to T9 parental lines, respectively. (**C** to **I**) Analysis of the location of pMD223 in Apa I restriction fragments of purified chromosomes. Chromosomes were separated by field inversion gel electrophoresis (FIGE) and stained with ethidium bromide after which appropriate chromosomes were excised in agarose. Blocks were incubated for 24 hours in 200 ml of restriction buffer containing bovine serum albumin (100 mg/ml) and 10 units of Apa I. Restriction fragments were separated by FIGE (*3*). Identical blots were initially hybridized to the DHFR-TS probe (C, F, and H) or pBSKS (D), and after stripping hybridized to the telomere probe (E, G, and I) (*3*). For the last probe, blots were washed with 1× standard saline citrate (SSC) containing 0.5% SDS at 65°C. FIGE conditions were as follows: first run, 20 hours, 1.2 V cm^{-1}, pulse time from 15 to 39 s; and second run, 3 hours, 1.5 V cm^{-1}, pulse time 10 to 14.5 s. In (G) there is a contaminating telomeric fragment of chromosome 11 (arrows). This is due to chromosome trapping during electrophoresis and is always observed when separating and analyzing *P. berghei* chromosomes of this size range (*11*). The telomeric fragment of increased size indicated by the arrow in (I), lane 2, demonstrates the frequent size polymorphism of the telomeric fragments. The additional bands hybridizing to the telomere probe in (I), lane 3, are from chromosomes 5 and 6, which comigrate because of the reduction in size of chromosome 7. For a detailed explanation, see (*11*). In (C), (D), and (E): lane 1, clone 15cy1, chromosome 7; lane 2, clone T6.2, chromosome 7; lane 3, clone T6.1, chromosome 7. In (F) and (G): lane 1, T7, chromosome 13/14; lane 2, T8, chromosome 13/14; lane 3, T9, chromosome 13/14; and lane 4, T9.1, chromosome 13/14. In (H) and (I): lane 1, high producer E, chromosome 7; lane 2, clone T9.1, chromosome 7; and lane 3, clone T9.2, chromosome 7.

some 7 carried by clone T9.2 were in all respects identical to those from the parental, sensitive clone, indicating that no obvious internal rearrangements had occurred. Densitometric examination of the blots probed with the DHFR-TS probe revealed that a single copy of the vector had integrated.

Integration of the vector was confirmed by Southern (DNA) blot analysis of Hind III–digested parasite DNA from the parental lines T6 through T9, demonstrating the presence of a predicted novel band of 3 kb hybridizing to the DHFR-TS locus probe. This band is indicative of vector integration into the 2.3-kb repeat (6) and was found for all the parental lines and clones analyzed (Fig. 2A). Plasmid rescue was also performed in which *Escherichia coli* was transformed with the same Hind III–digested, total parasite DNA from the T6 through T9 lines that had been circularized after digestion. Rescued plasmids contained the Hind III site of the target 2.3-kb repeat element in which integration had occurred (Fig. 2B), which was confirmed by DNA sequence analysis of the rescued plasmids (5). Taken together, the data are indicative of accurate, site-directed entry of the integration vector into the parasite genome. Analysis of clone T9.2 containing the truncated form of chromosome 7 indicated that integration had occurred through a reciprocal exchange, and the disposition of the integrated DNA was again characteristic of single-copy integration. The amount of DHFR-TS mRNA transcribed by the transformed parasites was on average 3.5 times that (range 2.5 to 4.0 times, 10 separate measurements) found in naturally resistant parasites carrying the Ser^{110}→Asn amino acid substitution in the allelic copy (5). This suggested that the integrated DHFR-TS gene was in fact transcriptionally upregulated rather than silenced, which might reflect a selective requirement for increased concentrations of DHFR-TS.

The 2.3-kb repeats are exclusively located in subtelomeric regions of *P. berghei* chromosomes, regions that have been shown to be transcriptionally inactive in *Plasmodium* (7) in a process that might result from an active silencing mechanism (8). Genes introduced into these regions were effectively expressed, thus refuting the possibility of a general silencing mechanism and pointing to a general paucity of genes in subtelomeric regions of *Plasmodium*. The observed limited distribution of integration sites may reflect either the local density of the integration target at the sites of integration or that only a subset of the possible integration sites will support gene expression in bloodstage parasites.

The integrated pMD223 was stable during asexual multiplication in the absence of pyrimethamine for 10 weeks (~70 generations) in all transformants tested (T6, T6.1, and T9.1). These parasites were analyzed as described above, and all the transformed parasites remained unaltered, being both highly drug resistant and positive in the diagnostic Hind III analysis of their genomic DNA (Fig. 2A). The stability was unexpected, as subtelomeric regions in *Saccharomyces cerevisiae* (9), trypanosomes (*10*), and *Plasmodium falciparum* (*11*) are known to be preferential sites for genomic rearrangements. Furthermore, the 2.3-kb repeat is involved in the generation of chromosome-size polymorphism (3) and recombination between nonhomologous chromosomes during mitosis in *P. berghei* (*12*).

These features of the 2.3-kb repeat unit may have different consequences for the stability of the inserted genes into these targets. It is possible that as a result of rearrangements involving the repeats, the inserted DNA may easily be mutated or lost, which we have not observed. Second, the inserted genes might be translocated (or duplicated) to other chromosomes, because of recombination between nonhomologous chromosomes involving or even mediated by the subtelomeric repeats (*11*). It will be of interest to observe if rearrangements occur during the obligatory meiosis in the zygote in the mosquito midgut.

This technique of site-directed integration of introduced DNA into the genome of malaria parasites brings us closer to being able to perform stable interruption, deletion, and modification of chosen endogenous genes of the parasite. In contrast to our previous report of episomal maintenance of introduced DNA (*2*), the data presented here show the site-directed insertion of pMD223 into the 2.3-kb tandem repeat cluster to be an effective and reproducible event. The results also support our interpretation of the earlier work, suggesting that propagation of circular DNA in *Plasmodium* is favored over integration of linear DNA. Thus, through removal of the circular form of the vector from the transfected DNA, integration events became observable. Moreover, the size of the flanking target sequences contained on the vector (800 and 1350 base pairs) was sufficient for the integration event to proceed with accuracy to specific sites.

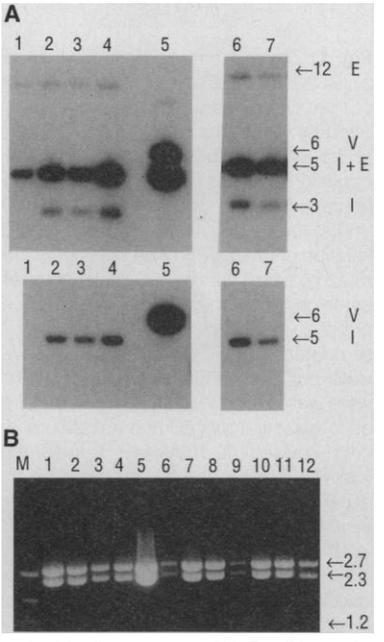

Fig. 2. Stable, targeted insertion of the integration vector into the 2.3-kb tandem repeat array occurred by homologous recombination. (**A**) Integration of linear pMD223 into the 2.3-kb repeat of *P. berghei*. Genomic DNA isolated from parasites from the transformed clones grown with (+) or without (−) drug pressure was digested with Hind III. DNA digests were size fractionated on 0.6% agarose gels, transferred to nylon filters, and analyzed by hybridization to the DHFR-TS locus probe (top panel) and to the pBSKS probe (bottom panel). Blots were washed with 0.1× SSC containing 0.5% SDS at 65°C. The following DNAs were used: lane 1, clone 15cy1; lane 2, clone T6.1+; lane 3, clone T6.2+; lane 4, clone T9.1+; lane 5, pMD223; lane 6, clone T6.1−; and lane 7, clone T9.1−. E, endogenous; I, integrated; and V, vector. Sizes of DNA fragments are indicated in kilobases. (**B**) Predicted rescue of the genomic Hind III restriction site adjacent to the site of integration. Total genomic DNA from parental lines T6 through T9 was digested with Hind III, diluted, and circularized with DNA ligase. The circularized DNA was then used to transform *E. coli*. Plasmid DNA was isolated from randomly picked colonies and cut with various restriction enzymes. Plasmids containing the Hind III–Eco RI 2.3-kb fragment could be rescued from the four parental lines and are distinguishable from original pMD223 (which might have either circularized on introduction to the parasite or spontaneously excised and religated) by the absence of the 1.2-kb band released by the double digestion. Hind III–Eco RI double digestion of plasmid DNA rescued from total DNA from: lanes 1 to 3, T6; lanes 4 and 5, T7; lanes 6 to 8, T8; lane 9 to 11, T9; and lane 12, Hind III–digested, diluted, and recircularized pMD223. M, marker.

REFERENCES AND NOTES

1. R. Goonewardene *et al.*, *Proc. Natl. Acad. Sci. U.S.A.* **90**, 5234 (1993); Y. Wu, C. D. Sifri, H.-H. Lei, X.-Z. Su, T. E. Wellems, *ibid.* **92**, 973 (1995).
2. M. R. van Dijk, A. P. Waters, C. J. Janse, *Science* **268**, 1358 (1995). The challenge dose of pyrimethamine was reduced from 10 mg per kilogram of body weight to 5 mg/kg for all experiments described.
3. M. Ponzi *et al.*, *Mol. Biochem. Parasitol.* **41**, 73 (1990).
4. M. R. van Dijk, G. A. McConkey, R. Vinkenoog, A. P. Waters, C. J. Janse, *ibid.* **68**, 167 (1994).
5. M. R. van Dijk, C. J. Janse, A. P. Waters, unpublished data.
6. Integration vector pMD223 was described previously (*2*). On digestion of *P. berghei* genomic DNA with Hind III, the following relevant fragments are generated; 2.3-kb-sized copies of the 2.3-kb repeat and 5- and 12-kb fragments of the genomic DHFR-TS locus. Insertion of linear pMD223 in the tandem repeat cluster leads to the introduction of a second copy of the genomic 5-kb Hind III DHFR-TS fragment and generation of a new fragment of 3 kb that will hybridize to the probe specific for the DHFR-TS locus. The hybridization to the 5-kb fragment therefore appears more intense. In addition,

Hind III digestion released another band of 5 kb, consisting largely of pBSKS vector sequences (Fig. 2A). Circularization of Hind III–digested genomic DNA containing pMD223 integrated by homologous recombination into a genomic array of 2.3-kb repeats will result in the formation of circular DNA elements that can be rescued by transformation back into *E. coli*. Digestion of rescued plasmid with Hind III and Eco RI demonstrates the rescue of the Hind III site adjacent to the site of integration and distinguishes between integrated and episomally maintained vector because the latter contains an additional 1.2-kb fragment (Fig. 2B). Sequence analysis confirmed the rescue of the Hind III site, which delineates the termini of the 2.3-kb repeat (*5*).

7. M. Lanzer, D. de Bruin, J. V. Ravetch, *Nature* **361**, 654 (1993).
8. M. Lanzer, K. Fischer, S. M. Le Blancq, *Mol. Biochem. Parasitol.* **70**, 1 (1995).
9. S. L. Gerring, C. Connelly, P. Hieter, *Methods Enzymol.* **194**, 57 (1991).
10. P. Borst and D. R. Greaves, *Science* **235**, 658 (1987).
11. L. G. Pologe and J. V. Ravetch, *Cell* **55**, 869 (1988); L. G. Pologe, D. de Bruin, J. V. Ravetch, *Mol. Cell. Biol.* **10**, 3243 (1990); A. Scherf *et al.*, *EMBO J.* **11**, 2293 (1992).
12. T. Pace *et al.*, *Mol. Cell. Biol.* **10**, 6759 (1990); C. J. Janse, J. Ramesar, B. Mons, *Nucleic Acids Res.* **20**, 581 (1992); E. Dore, T. Pace, M. Ponzi, L. Picci, C. Frontali, *Mol. Cell. Biol.* **10**, 2423 (1990); M. Ponzi *et al.*, *Nucleic Acids Res.* **20**, 4491 (1992).
13. During the course of this work we became aware of similar work with asexual bloodstage forms of the human malaria parasite, *P. falciparum*. Plasmid DNA has been successfully introduced into the *P. falciparum* genome in a site-specific manner with DHFR-TS genes from either *P. falciparum* or *Toxoplasma gondii*. A manuscript describing this work is now in press (Y. Wu, L. A. Kirkman, T. E. Wellems, *Proc. Natl. Acad. Sci. U.S.A.*, in press.
14. We thank J. Ramesar and J. Kos for technical assistance, the yeast genetics group in the Institute of Molecular Plant Sciences at Leiden for consideration of our work, R. Vinkenoog and R. E. Sinden for discussions, G. van Dam for curve fitting, and H. A. del Portillo for critical reading of the manuscript. This work was supported by grants from the European Union program "Science and Technology for Development" (contract TS3*-CT92-0116) and the United Nations Development Program–World Bank–World Health Organization Special Programme in Research and Training in Tropical Diseases (contract 940351).

11 August 1995; accepted 21 November 1995

IRS-1–Mediated Inhibition of Insulin Receptor Tyrosine Kinase Activity in TNF-α– and Obesity-Induced Insulin Resistance

Gökhan S. Hotamisligil,* Pascal Peraldi, Adriane Budavari, Ramsey Ellis, Morris F. White, Bruce M. Spiegelman†

Tumor necrosis factor–α (TNF-α) is an important mediator of insulin resistance in obesity and diabetes through its ability to decrease the tyrosine kinase activity of the insulin receptor (IR). Treatment of cultured murine adipocytes with TNF-α was shown to induce serine phosphorylation of insulin receptor substrate 1 (IRS-1) and convert IRS-1 into an inhibitor of the IR tyrosine kinase activity in vitro. Myeloid 32D cells, which lack endogenous IRS-1, were resistant to TNF-α–mediated inhibition of IR signaling, whereas transfected 32D cells that express IRS-1 were very sensitive to this effect of TNF-α. An inhibitory form of IRS-1 was observed in muscle and fat tissues from obese rats. These results indicate that TNF-α induces insulin resistance through an unexpected action of IRS-1 to attenuate insulin receptor signaling.

Insulin resistance, a smaller than normal response to a given amount of insulin, is a common pathological state frequently associated with a number of diseases, including chronic infection, cancer, and obesity (*1*, *2*). In the case of obesity, insulin resistance is a ubiquitous correlate and predisposes the obese individual to the most deleterious consequences of this condition, such as cardiovascular complications and, especially, non–insulin-dependent diabetes mellitus (NIDDM) (*3*). However, the molecular mechanisms responsible for the development of insulin resistance in obesity are not well understood.

Overexpression of TNF-α from adipose tissue is a common feature of many different rodent models of obesity (*4*, *5*). Increased TNF-α expression in adipose tissue is also present in human obesity and correlates with the extent of obesity and the level of hyperinsulinemia, an indirect measure of insulin resistance (*6*). Moreover, neutralization of TNF-α in obese and insulin-resistant rats improves IR signaling and insulin sensitivity of peripheral tissues, demonstrating that TNF-α interferes with insulin action in this disease (*4*, *7*).

Binding of insulin stimulates the intrinsic tyrosine kinase of the IR, which results in autophosphorylation of the β subunits on tyrosine residues and subsequent phosphorylation of insulin receptor substrate 1 (IRS-1) (*8*). One mechanism by which TNF-α interferes with insulin action is through its ability to inhibit these proximal steps in IR signaling in both cultured cells and whole animals (*7*, *9*, *10*). Treatment of adipose cells with TNF-α produces a decrease in both insulin-stimulated IR autophosphorylation and subsequent tyrosine phosphorylation of IRS-1 (*9*). Similar results have also been obtained with cultured hepatoma cells, muscle cells, and fibroblasts (*10*–*12*). The time course of TNF-α effects on IR signaling, however, is variable in these different cell types.

TNF-α initiates a cascade of signal transduction events through the activation of multiple protein kinases (*13*). We therefore examined whether TNF-α also induces alterations in the phosphorylation of IR or IRS-1 or both. We metabolically labeled 3T3-F442A adipocytes with [^{32}P]orthophosphate and determined the phosphorylation patterns of IR and IRS-1 before and after TNF-α treatment. As expected, insulin-stimulated autophosphorylation of the IR and phosphorylation of IRS-1 were reduced in TNF-α–treated adipocytes (Fig. 1A). An increase (≈threefold) in IRS-1 phosphorylation was apparent in TNF-α–treated cells compared with the controls. There was no detectable tyrosine phosphorylation of IRS-1 without insulin stimulation. However, we observed two proteins, p120 and p210, that were tyrosine phosphorylated upon TNF-α stimulation. The identity of these proteins is currently unknown. Phosphoamino acid analysis of IRS-1 isolated from control and TNF-α–treated cells revealed that the TNF-α–induced phosphorylation of IRS-1 occurred exclusively on serine residues (Fig. 1C). No phosphorylation of IRS-1 was detected in control adipocytes.

Phosphorylation of IRS-1 on serine and threonine residues interferes with the subsequent insulin-stimulated tyrosine phosphorylation of IRS-1 by the IR (*14*). Treatment of adipocytes with okadaic acid, a protein phosphatase inhibitor, which results in increased serine and threonine phosphorylation of IRS-1, also reduces the capacity of IRS-1 to be phosphorylated by the IR and induces a state of cellular insulin resistance (*14*). We therefore asked whether the serine-phosphorylated IRS-1 from TNF-α–treated cells can be phosphorylated normally by the IR after insulin stimulation. IRS-1 was immunoprecipitated from control and TNF-α–treated cells and incorporated in an in vitro kinase assay with par-

G. S. Hotamisligil, P. Peraldi, A. Budavari, R. Ellis, B. M. Spiegelman, Department of Cellular and Molecular Biology, Dana-Farber Cancer Institute, and Department of Cell Biology, Harvard Medical School, 44 Binney Street, Boston, MA 02115, USA.
M. F. White, Joslin Diabetes Center and Department of Medicine, Harvard Medical School, Boston, MA 02215, USA.

*Present address: Department of Nutrition, Harvard School of Public Health, 665 Huntington Avenue, Boston, MA 02115, USA.
†To whom correspondence should be addressed. E-mail: bruce_spiegelman@dfci.harvard.edu